Microchemical Journal 220 (2026) 116339

Contents lists available at ScienceDirect

Microchemical Journal

journal homepage: www.elsevier.com/locate/microc

Development of thio-rich double-linker MIL-53 (Fe) as sorbent in pipette-tip micro solid phase extraction method for determination of Lead and Cadmium in environmental water samples

Qaissar Guti Omo [a], Soleyman Moinfar [b,c,*]

[a] Environmental Science Department, University of Zakho, College of Science, Zakho, Iraq
[b] Chemical analysis research center, Scientific Research Center, University of Zakho, Zakho, Iraq
[c] Department of Basic Sciences, College of Pharmacy, Nawroz University, Duhok, Iraq

ARTICLE INFO

Keywords:
Lead
Cadmium
Thio-rich-double linker MIL-53(Fe)
Pipette tip micro solid phase extraction
Graphite furnace atomic absorption spectrometry
Water

ABSTRACT

Metal-organic framework (MOF)are a great advanced adsorption material for solid-phase extraction due to the structure modifications with functional groups like sulfur that enhance the adsorption of heavy metals. A new sulfur-rich three-dimensional two-linker MOF (MIL-53(Fe)) was synthesized by grafting 2-mercapto-2-thiazoline sulfur and nitrogen as the second linker and then applied as an adsorbent in pipette tip micro solid-phase extraction (PT-μSPE) for the determination of Pb (II) and Cd (II) in environmental water samples. The MOFs were characterized by FTIR, XRD, TGA, BET, and SEM, which provide evidence for its framework, thermal stability, surface area, and morphology. Optimizations of extraction parameters such as pH, sample volume, volume of desorption solvent, and acidity of desorption solvent were made to improve the analytical performance. Optimizations of extraction parameters such as pH, sample volume, volume of desorption solvent, and acidity of desorption solvent were made to improve the analytical performance. In the optimal conditions, higher surface area and adsorbent capacity per adsorbent weight were obtained for the newly synthesized adsorbent containing sulfur and nitrogen when compared to MIL-53(Fe). The linearity range of the developed method was 0.2–55 μg L^{-1} for Pb (II) and 0.04–20 μg L^{-1} for Cd (II), while it displayed exceptional linearity ($r^2 > 0.99$) and acceptable precision (RSD% $\leq$ 6.3). Thio-rich double-linker MIL-53 (Fe) as adsorbent in μSPE was applied for analysis spiked river, lake, groundwater, and wastewater samples with Pb (II) concentrations ranging from 5.0 to 20.0 μg L^{-1} and Cd (II) concentrations from 1.0 to 5.0 μg L^{-1}, as well as standard reference materials. The results suggest that the double linker MIL-53(Fe) bearing thio-rich may offer greater adsorption capacity for Pb (II) and Cd (II) with a significantly lower detection limit compared to the original MIL-53(Fe).

1. Introduction

The greater toxicity, bioaccumulation potential, and persisting nature in the environment render these metals a public health threat and an environmental concern in water sources [1]. Among the said contaminants, Pb (II) and Cd (II) are most significant threats to human life since they entail the risk of neurological disorders, organ damage, and cancer even at very low levels of exposure [2]. Owing to rapid industrialization, heavy metals are continuously discharging into the water bodies through the industrial effluents, mining, and poor waste management [3]. The metals are harmful to both fauna and man; therefore, Pb (II) and Cd (II) should be removed from industrial effluents before they can find their way into surface waters [4]. It is now even more dangerous than the second most toxic metal after lead. Lead has been thrown out due to human activities, such as automobiles, factories, and battery manufacture, causing huge risks to both human health and the environment. [5]. According to WHO standards, the maximum permissible Pb (II) concentration allowed in drinking water is 10.0 μg L^{-1} [6]. Toxic Cd has been recognized as one of the major environmental contaminate [7,8]. Its presence in lakes makes cadmium a very serious pollutant that endangers both aquatic life and water quality due to its extremely long biological half-life and toxicity [9]. USEPA establishes the permissible value of cadmium in drinking water at 3.0 μg L^{-1} [10]. Analytical techniques of ICP-MS [11], flame atomic absorption spectrometry (FAAS) [12] and graphite furnace atomic absorption spectrometry (GFAAS) [13] can be used in the detection of metal ions. You

* Corresponding author.
E-mail address: soleiman_moinfar@yahoo.com (S. Moinfar).

https://doi.org/10.1016/j.microc.2025.116339
Received 23 July 2025; Received in revised form 22 November 2025; Accepted 24 November 2025
Available online 30 November 2025

cannot really detect trace heavy metals in real samples through any of the analytical techniques mentioned above, as they all have their limitations, including sample matrix effects and limited detector sensitivity [14,15]. Therefore, techniques for extraction and determination of these dangerous metals have been needed to be highly effective and sensitive in the prospect of allowing a safe water supply and public health benefits. Different methods of pretreatment such as liquid phase microextraction (LPME) [16,17], liquid-liquid extraction (LLE) [18], and solid phase extraction (SPE) [19] have been employed to extract and preconcentrate heavy metal ions from different kinds of sample matrices. Other advantages of SPE over other extraction techniques include process reusability, simplicity, so-called high preconcentration factors, low consumption of organic solvents, and high adsorption capacity. Different types of SPE are still in operation today [20,21]. The concept was further developed into a miniaturized and simpler method of extraction, such as pipette tip micro-SPE (PT-μSPE), with advantages such as ease of use, small consumption of sample and solvents, and the ability to handle great numbers of samples processed through pipette tips [22]. The success of μ-SPE greatly depends on the properties of the sorbent material, which must have high binding affinities, large surface area, and selective adsorption. In this way, MOFs have turned adsorptive separation methods upside down with their porosity which is tunable and huge surface area, and the last multifunctionality feather in the cap [23]. MOFs consist of metal clusters coordinated to the organic linkers which permit precise structural design and modification to enhance their adsorption capability [24]. Functional groups in the MOFs will also induce an improved selective adsorption toward specific target analytes that can be successfully applied for heavy metal extraction [25]. The performance of the property under consideration in regard to improved adsorption performance can be successfully enhanced by functionalization with appropriate functional groups or structural defect creation [26]. The Pb (II), Cd (II), and Hg (II) are the most frequently used species for effective removal with sulfur-functionalized materials, owing to the strong binding affinity of the sulfide groups toward the soft heavy-metal entities. Normally sulfur has been incorporated into new adsorbents derived from a MOF using two approaches: selection of sulfur-containing ligands to act as linkers for in-situ or post-synthesis functionalization of the new MOFs [27]. These ligands are now exchanged in the mixed-ligand MOFs and are expected to introduce some new functional groups. The latter developed has sulfur-functionalized MOF (Fe_3O_4 @UiO-66-SH) using 2,5-dimercaptoterephthalic acid as the ligand for mercury profiling in water [27]. Post-synthetic functionalization of UiO-66-NH_2 via 2,5-Dimercapto-1,3,4-thiadiazole was utilized to remove Hg(II) [28]. A mixed-ligand MOF (DUT-67-SH) has been successfully constructed by the combination of 2,5-thiophenedicarboxylic acid and thioglycolic acid for the removal of Hg(II) [29]. Xu et al. [30] went further to the preparation of MOF-808-SD via a mixture of tetracarboxyporphyrin and trimesic acid and realized the high adsorption capacity of Hg (II). Multi-ligand thiol functionalized defective Zr-MOFs were constructed from 2,3-dimercaptosuccinic acid and mercaptosuccinic acid for the removal of Hg (II), Cd (II), and Pb (II) [26]. Post-synthetic modification of MIL-100 (Fe) via ethanedithiol was used for the removal of Hg (II), Cd (II), and Pb (II), which is the only Fe-containing MOF reported in this field [31]. The use of MOF and PT-μSPE provides a simple analytical technique for the determination of heavy metals in various samples. This type of application is limited by the difficulty in preparing a suitable MOF that can adsorb heavy metals with high capacity; a number of recent studies have been conducted to achieve this goal [32]. The use of a Zr-MOF in PT-μSPE for the extraction of Hg (II) from fish samples has been reported [33]. In addition, another study reported the determination of cadmium using amino-functionalized-Zr-MOF in PT-μSPE, which showed an increased selectivity compared to a previous study conducted with Zr-MOF [34].

In this study, defective thio-rich linker MIL-53(Fe) was synthesized through a one-pot reaction by mixing 2-mercapto-2-thiazoline and the original MIL-53(Fe) backbone. By adding sulfur-containing linkers to the backbone of the MOF, the synthesis becomes simpler, with less solvent consumption (single-step synthesis and washing without post-synthesis modification) and with chemical stability evidenced by the achieved high reusability. Synthesized functionalized MOFs, which were applied to adsorb some of metals, have been reported in the critical review recently [35] however, this is the first time that a thioether 2-mercapto-2-thiazoline with two sulfur groups was incorporated into MIL-53(Fe) for solid-phase extraction as an adsorbent for enriching and detecting Pb (II) and Cd (II) metals in water samples. The novel synthesized double-linkers was incorporated as the sorbent within pipette tips and optimized several analytical parameters, including pH of sample, sample and desorption solvent volumes, and acid concentration of desorption solvent using thio-rich double-linker MIL-53(Fe) as the sorbent. Then, extracted Pb (II) and Cd (II) were quantified by GF-AAS. The adsorption capability and extraction performance of the thio-rich double link MIL-53(Fe) for Pb (II) and Cd (II) were thus evaluated and compared in detail with MIL-53(Fe). Results confirmed that the Pb (II) and Cd (II) adsorption capabilities were augmented by the presence of sulfur in the thio-rich double-linker, while the extraction efficiency also was improved with increasing total pore volume.

2. Material and method

2.1. Materials

We got our *N*,*N*-Dimethylformamide (DMF, 99.8 % purity) from Scharlau in Spain. Iron (III) chloride hexahydrate ($FeCl_3{\cdot}6H_2O$, 97 % purity), terephthalic acid ($C_6H_4(COOH)_2$, TPA $\geq$ 98 % purity), and sodium nitrate ($NaNO_3$, 99 % purity) were provided by Beachem Chemo Pharma, France. The 2-mercapto-2-thiazoline (C3H5NS2, 2-MT at 97 % purity) was purchased from Fluka AG, Switzerland. Methanol of the highest purity (99.9 %) and nitric acid (HNO_3 65 %) were from Merck, Germany. Sodium hydroxide (NaOH $\geq$98 % purity) was purchased from Karlsruhe, Germany. A stock solution containing 1000 mg L^{-1} of Cd (II) and Pb (II) was obtained from Merck, Darmstadt, Germany. The standard solutions of the metals in question were prepared in ultrapure water and HNO_3 (0.2 M).

2.2. Apparatus

Kindly see the supplemental information for specific information regarding the Apparatus.

2.3. GF-AAS conditions

Also included in the system were an atomic absorption spectrophotometer, PinAAcle 900 T (PerkinElmer, USA), WinLab32 software, and a highly efficient optical system, specifically designed to maintain suitable signal-to-noise ratios. Argon gas (99.999 % purity, Air Products, UK) was the inert gas used. Heated injection methods were employed for the analyses of Pb (II) and Cd (II). An autosampler automatically injected 15.0 μL of extraction solvent into the atomizer for measurement. The experimental conditions and preferred graphite furnace temperature program used in this study are summarized in Table 1.

2.4. Synthesis of MIL-53 (Fe)

The synthesis of MIL-53 (Fe) was performed as previously established. The mixture consisted of 9.63 mmoles of terephthalic acid, 7.39 mmoles of ($FeCl_3$-$6H_2O$), and 20.0 mL of *N*,*N*-dimethylformamide (DMF), and it was vigorously stirred for 1 h. The mixture was transferred, as shown in Fig. 1a, to a Teflon-lined stainless-steel autoclave and heated at 150 °C for 16 [36]. After the reaction, cool down the autoclave from that temperature to room temperature. This is followed by centrifugation at 6000 rpm for 5 min to separate the supernatant from the yellow precipitate. The resulting material was washed with DMF

Table 1
Operating conditions of graphite furnace temperature program for determination of Pb (II) and Cd (II).

Instrumental conditions			
Wavelength/nm			Cd:228.8, Pb:283.3
Spectral bandwidth/nm			0.7
Lamp current/mA			8 and 10
Integration mode			Peak height
Sample volume/μL			1 5
Background correction			D2
Chemical modifier			0.05 mg NH4H2PO4 + 0.003 mg Mg(NO3)2
Graphite furnace temperature program			
Step	Temperature (°C), time (sec)		Argon flow rate (L min^{-1})
	Cd	Pb	
Dry1	110	110	0.25
Dry2	130	130	0.25
Pyrolysis	500	850	0.25
Atomization	1500	1600	0
Clean	2450	2450	0.25

under stirring for 24 h. This was again followed by centrifugation of the product at 6000 rpm for 5 min, after which it was subjected to methanol washing, repeating this washing step thrice. Finally, the purified MIL-53 (Fe) ended drying in an ordinary oven at 100 °C for 12 h.

2.5. Synthesis of thio-rich-double linker MIL-53 (Fe)

For synthesis of thio-rich-double linker MIL-53 (Fe), a similar synthesis method has been utilized for MIL-53(Fe), but with a few changes from the original. The normal procedure used was a combination of 6.7 mmol of terephthalic acid, 7.39 mmol of $FeCl_3.6H_2O$, and 3.01 mmol of 2-mercapto-2-thiazoline (2-MT) and mixed in 20.0 mL DMF. As shown in Fig. 1 a, the stirrer was stirred with great intensity for 1 h. After this, it was placed inside a Teflon-lined stainless-steel autoclave and heated at 150 for 16 h. After the reaction, the autoclave is cooled down to room temperature. The precipitate of the thio-rich double-linker MIL-53(Fe) was separated from the reaction mixture by centrifugation. The obtained solid was then washed with DMF two times and left stirring for 24 h to desorb the unreacted terephthalic acid adsorbed within the MOF pores. MOFs powder was removed from the solution by centrifugation at 6000 rpm for five minutes. This product was then washed extensively with methanol (3 × 50 mL), followed by vacuum drying at 100 °C for 12 h.

2.6. Preparation of pipette tip for SPE

18.0 mg of thio-rich double-linker MIL-53 (Fe) sorbent was filled uniformly on filter paper and was placed into a 1 mL pipette tip. This pipette tip was connected to a 60 mL syringe, as illustrated in Fig. 1b. Conditioning of the packed sorbent was done by washing with 2.0 mL of 0.2 mol L^{-1} HNO_3. After preparation, the micropipette-tip micro-SPE was used for the pre-concentration of Pb (II) and Cd (II) ions from the water sample.

2.7. Preparation of samples

Kindly see the supplemental information for specific information regarding the preparation of samples.

2.8. Extraction procedure

All samples were adjusted to a pH of 7.5 with the addition of a 0.01 mol L^{-1} solution of HNO_3 and a 0.01 mol L^{-1} solution of NaOH for the extraction of Pb (II). Next, 60.0 mL of either the non-spiked or spiked samples with the target ion were passed separately through a pipette tip packed with the thio-rich double-linker MIL-53(Fe) sorbent (flow rate 3 mL min^{-1}). Desorption of the retained Pb (II) was then carried out with 2.5 mL of HNO_3 (0.3 mol L^{-1}) as the eluting solvent. In the case of Cd (II), the solution was adjusted to pH 8.5 with 0.01 mol L^{-1} HNO_3 and 0.01 mol L^{-1} NaOH. Then, 60.0 mL of the spiked or non-spiked samples were passed through the pipette tip filled with sorbent and subsequently eluted with 2.0 mL of HNO_3 (0.3 mol L^{-1}). Finally, the assembled desorption solvent of the extracted Cd (II) and Pb (II) was analyzed by the graphite furnace atomic absorption spectrometer (GFAAS).

2.9. Adsorption experiments

Adsorption experiments under optimum conditions, adding 40.0 mg of thio-rich double-linker MIL-53 to 60.0 mL of Cd (II) and Pb (II) solutions with known concentrations, were stirred for 2 h. The synthesized adsorbent was then separated from the supernatant by centrifugation, and the concentration of Cd (II) and Pb (II) in the supernatant was determined using GF-AAS. The adsorption capacity (Qe, mg·g^{-1}) can then be calculated from the following equation:

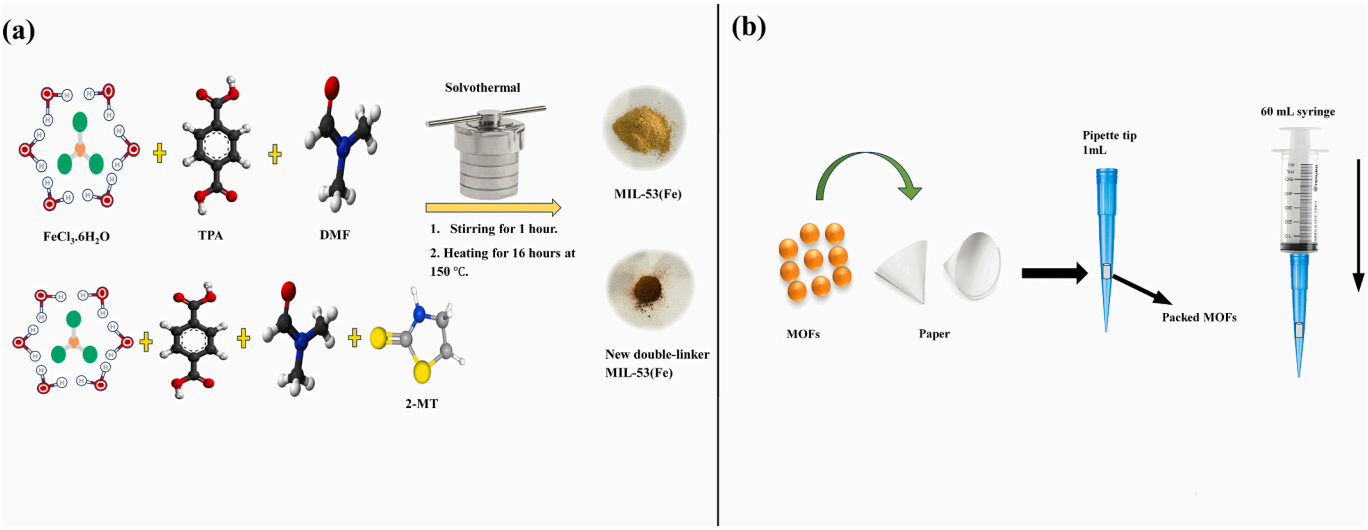

Fig. 1. (a) The visualized procedure of synthesizing MIL-53(Fe) MOF and the newly developed double-linker MIL-53 (Fe). (b) A schematic preparation of the MOF packing process in pipette tips used for PT-μSPE fabrication.

$$Q_e = \frac{(C_0 - C_e)V}{m}$$

Here, Qe (mg g^{-1}) defines the volume at which saturated adsorption occurs (equilibrium); V (L) is the volume of the solution; Co defines the initial concentration of metals at the beginning of the process, while Ce defines the concentration of metals after equilibrium; and, finally, m (g) represents the mass of adsorbent [37].

3. Results and discussion

3.1. Characterization

We characterized the synthesized materials' surface morphology and particle size through scanning electron microscopy techniques. Fig. 2a and b show that pristine MIL-53(Fe) possesses a crystalline morphology extending from rod-like to plate-like and irregular forms with aggregated particles. The bigger crystals are crowned by smaller spherical nanoparticles, with particle size measurement of 99.73 and 107.4 nm. This gives rise to a non-uniform emerging surface, making the access to active adsorption sites difficult [38]. The thio-rich double-linker MIL-53 (Fe) in SEM images provides a diametrically opposite presentation, as seen in Fig. 2c and d; otherwise, there is marked change in shape together with other surface characteristics of the particle. The particles are shaped like spheres and tightly packed with a grainy and hole-ridden structure. The particles are smaller, measuring to be around 64.49 and 94.43 nm. The size reduction in the particles and the improved morphological uniformity may have happened due to the introduction of the *sec*ond linker, 2-mercapto-2-thiazoline, which is likely sulfur and nitrogen-assisted in controlling nucleation during the entire synthesis reaction.

The EDX analysis, elemental quantitative data table and elemental mapping of the thio-rich double-linker MIL-53 (Fe) are shown in Fig. 3. The percentage of the index elements is indicated by the EDX spectrum in the thio-rich double-linker MIL-53 (Fe) (S = 4.3 %, Fe = 17.7 %, *N* = 1 %, C = 31.2 %, O = 45.8 %). Furthermore, in the thio-rich double-linker MIL-53 (Fe), a uniform distribution of elements was revealed, indicating the contribution of N and S in the MOF structure. Fig. 3 shows the uniform distribution of elements in the prepared two-linker MOF. The EDX elemental analysis of the synthesized thio-rich double-linker MIL-53 (Fe), confirmed the presence of sulfur and nitrogen, with S and N being the abundant atoms.

In the FTIR spectrum of the MIL-53(Fe), characteristic vibrational bands corresponding to its functional groups and structural components can be seen. As shown in Fig. 4a, the broad band centered at 3430 cm^{-1} has been assigned to stretching vibrations of the hydroxyl (-OH) groups, presumably deriving from either adsorbed water molecules within the MOF pores or to intermolecular hydrogen bonding within the framework [39]. The peaks at 1676 and 1538 cm^{-1} correspond to the asymmetric and symmetric stretching vibrational modes of the carboxylate ($-COO^-$) groups, respectively, which also confirm the coordination of the organic linker, terephthalic acid, to the Fe centers within the MOF structure. In addition, another pair of aromatic and C—H vibrational modes are found at 1388 and 1018 as well as 820 cm^{-1} due to C—O stretching vibrations, C—H bending of an aromatic ring and C—H out-of-plane bending due to the benzene of the linker methyl terephthalate. Also found are the metal-oxygen (Fe—O) stretching vibrations at 750 and 528 cm-^{1}, which establish the coordination of Fe clusters with the organic linker in the framework of the MOF [36]. Unlike this kind of feature in Fig. 4a, the FTIR spectrum for this thio-rich

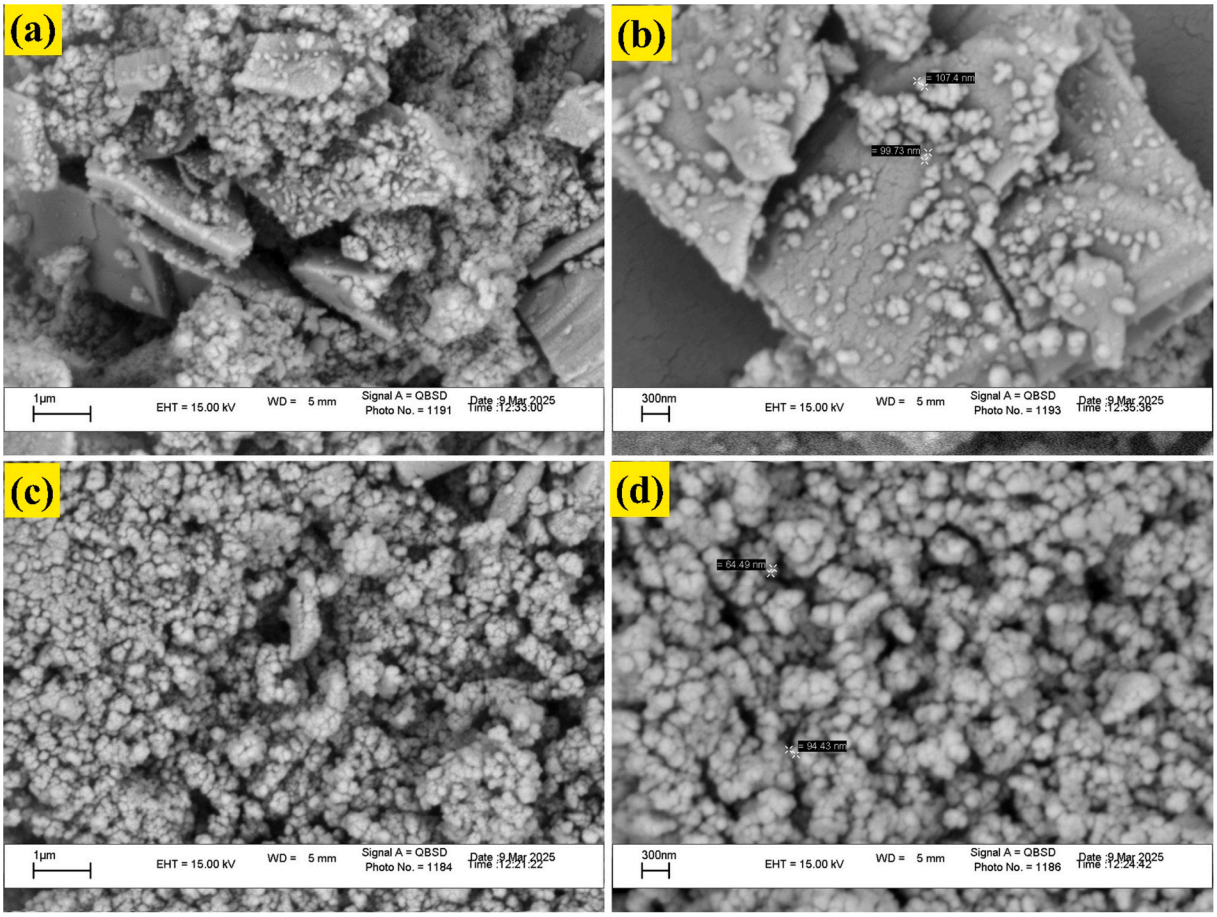

Fig. 2. Scanning electron microscopy (SEM) images of (a, b) MIL-53 (Fe) and (c, d) thio-rich double-linker MIL-53 (Fe).

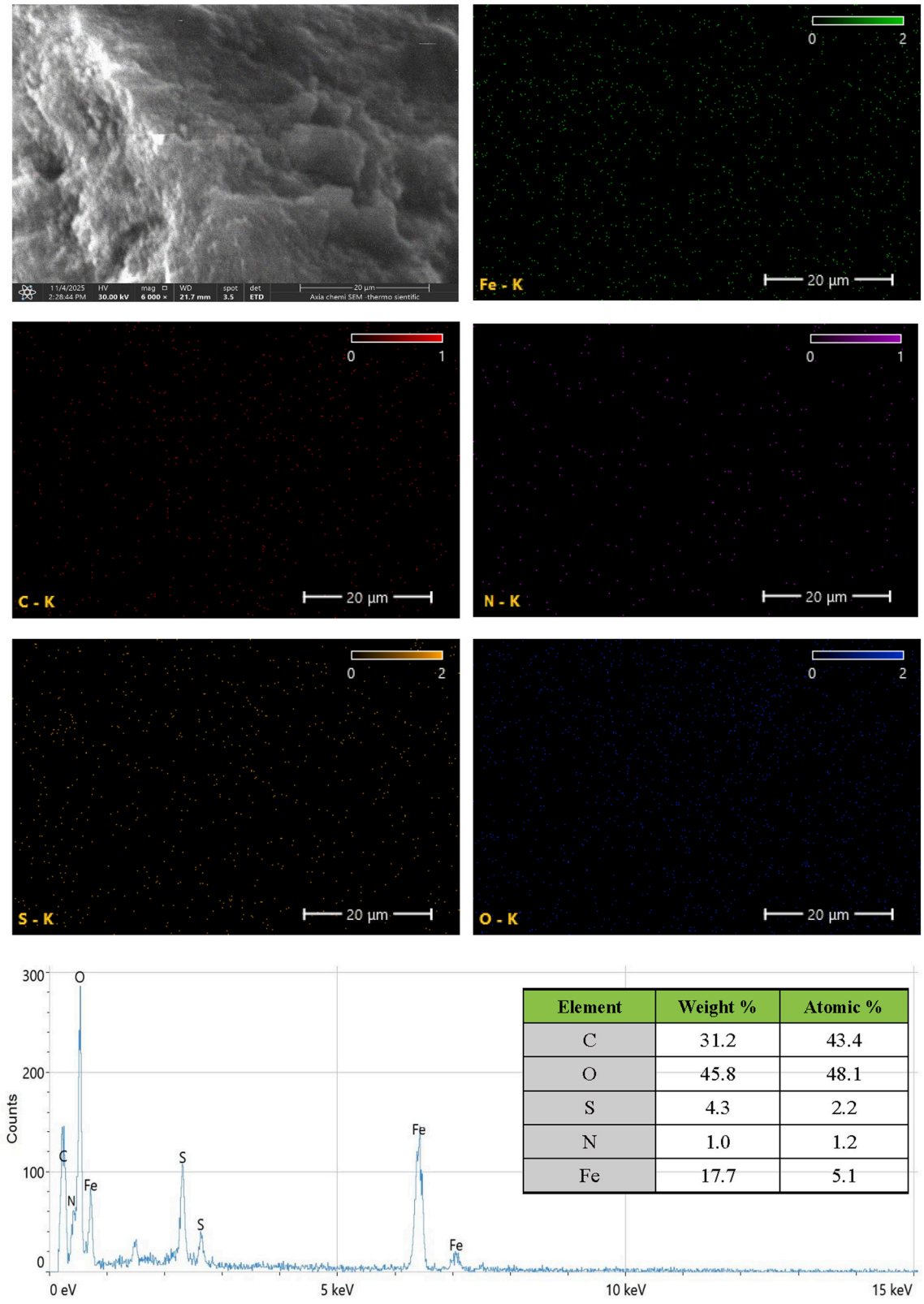

Element	Weight %	Atomic %
C	31.2	43.4
O	45.8	48.1
S	4.3	2.2
N	1.0	1.2
Fe	17.7	5.1

Fig. 3. EDX spectrum and elemental mapping for thio-rich double-linker MIL-53 (Fe).

double-linker MIL-53 (Fe) exhibited a lot of significant vibrational shifts, which could be considered as solid proof for the inclusion of 2-mercapto-2-thiazoline in the framework of the MOF. A clear peak at 3436 cm^{-1} suggests O—H stretching, which may arise from hydroxyl groups or from physically adsorbed water molecules present inside the MIL-53(Fe) framework. The small downshift when compared to pristine MIL-53 (Fe) at 3430 cm^{-1} indicates some alteration in the hydrogen bonding, which probably is due to the incorporation of 2-mercapto-2-thiazoline, which in turn can provide some additional anchoring. The asymmetric ($-COO^{-}$) stretch at 1582 cm^{-1} and the symmetric stretch at 1396 cm^{-1}

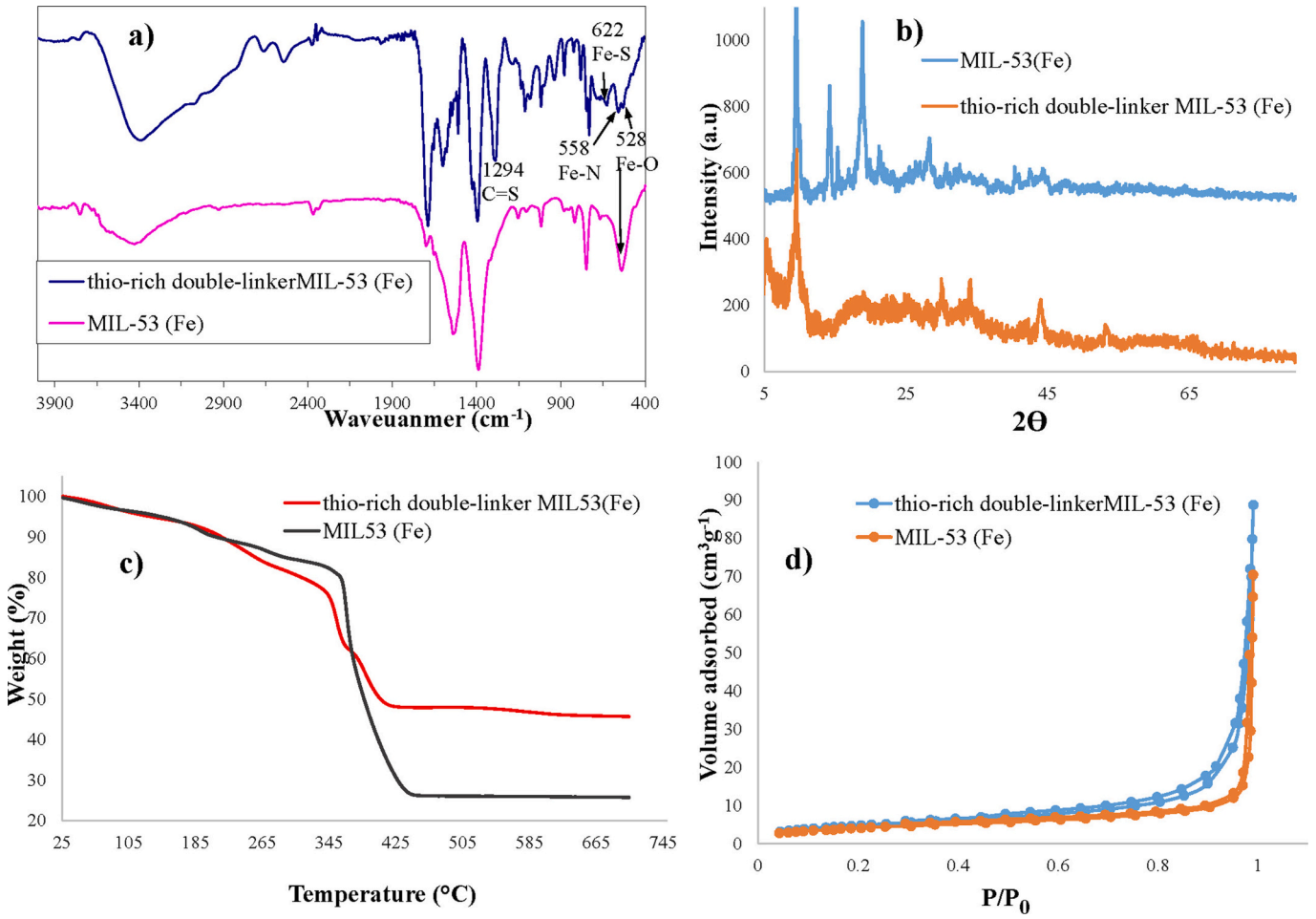

Fig. 4. (a) FTIR spectr, (b) XRD patterns, (c) TGA, (d) N2 adsorption-desorption isotherms of MIL-53(Fe) and thio-rich double-linker MIL-53(Fe).

are both downshifting from the values corresponding to the carboxylate (-COO$^-$) stretches at 1676 cm^{-1} and 1388 cm^{-1} of MIL-53(Fe). The shifts suggest that coordination of metals was altered due to the terephthalic acid linker-2-mercapto-2-thiazoline interaction. Novel peaks were found to be appeared with characteristic frequencies; one peak around 558 cm^{-1} due to Fe—N bending vibrations [40] and the other at 622 cm^{-1} due to Fe—S stretching [41]. In addition, C═S stretches at 1294 cm^{-1} supporting the presence of thiazoline ring and sulfur-containing functional groups [42]. In the same way, the greatest peaks studied at 748 cm^{-1} are due to the C—H out-of-plane distortion of the benzene ring of terephthalic acid, an attribute whose intensity is slightly modified with variation in the π- π stacking interactions.

Results from the characterization of X-ray diffraction study information reveal the core attributes pertaining to pure and modified types of thio-rich double-linker MIL-53(Fe) samples along with their variable degrees of crystallinity and functionality. Significant peaks of MIL-53 (Fe) samples can be seen at the following angles: 9.42, 14.17, 18.77, 21.12, and 28.22 (2θ) as depicted in Fig. 4b. The peaks were characteristic of the diffraction pattern of MIL-53(Fe) which confirmed that it has been synthesized in an efficient fashion in well-crystallized form [43]. However, in thio-rich double-linker MIL-53(Fe), there was much lowering of the intensity of these characteristic peaks implying that structural alteration, partial amorphization, or the formation of a new phase possibly occurs. The core of MIL-53(Fe) which has been functionalized with 2-mercapto-2-thiazoline would appear to possess slightly less crystallinity. This modification reduces the sharpness of peaks, thereby diminishing long-range order and giving rise to the observed loss in crystallinity [44]. The wide background in the diffraction pattern indicates either an amorphous phase or a low degree of crystallinity; the small remaining peaks indicate that some amount of crystallinity still exists, notwithstanding the apparent changes in structure. The increased intensity of the baseline points to the likely occurrence of disorder, defects, or some surface modification resulting from interactions between the iron clusters and the sulfur functional groups of 2-mercapto-2-thiazoline. The most striking peak in the double linker MIL-53(Fe) appears quite near to the angle 2θ = 9.5° as expected, seen from Fig. 4b and the other observable peaks at 12°, 18°, and 25°. Compared to MIL-53(Fe), some sharp peaks appear to have either disappeared or broadened, thus further confirming the changes in the framework. These changes in intensity of peaks, disappearance, or broadening indicate variations in the framework, which might be due to doping, induced distortions or even functionalization. Baseline intensity can also be taken as an indication of defects, increased porosity, or formation of amorphous phase contribution.

The TGA curve for both MIL-53(Fe) and thio-rich double-linker MIL-53(Fe), as depicted in Fig. 4c, represents thermal decomposition behavior with rising temperature. Both materials have a slight weight loss in the initial temperature range of approximately 50 to 200 °C, due to the evaporation of physically adsorbed water and residual solvents trapped in the pores. Thereafter, a significant weight loss of pristine MIL-53(Fe) occurs in the range of 300–450 °C owing to the degradation of its organic linker and deterioration of its structure [45]. Fig. 4c exhibits primary decomposition occurring between 360 and 450 °C. About 25 % of the mass remains, resulting from iron oxide residue formation. In MIL-53 (Fe), on the contrary, 2-mercapto-2-thiazoline was combined with terephthalic acid as a second ligand and its thermal stability was

determined by thermogravimetric analysis (TGA) as shown in Fig. 4c. The TGA curve exhibits a two-step weight loss pattern. The first stage, occurring from ambient temperature up to about 370 °C, involved the loss of residual DMF and water, as well as the degradation of the low-temperature 2-mercapto-2-thiazoline ligand. This sulfur and nitrogen-containing heterocyclic linker undergoes early degradation due to the cleavage-prone nature of its C—S or N—S bond, smaller molecular size, and weaker coordination to Fe (III). This initial event constituted about 40 % of the entire weight loss. The second range ranging from 370 °C up to 420 °C indicates the decomposition of a more thermostable linker, terephthalic acid, contributing to an additional 13 % weight loss. The other 45 % mass loss after 440 °C is likely due to the formation of iron oxide. The two-step nature of the weight loss indicates different thermal behavior for the two ligands included and affirms their successful incorporation into the MIL-53(Fe).

The Braunauer – Emmet - Teller method finds a widespread use in determining the surface area of different metal-organic frameworks (MOFs), which, by the way, are characterized by their high porosity. However, some complications arise when applying the BET theory to the MOFs because of their complex pore structures and variable surface chemistry [46]. All the samples were heat treated under vacuum at 300 °C for 3 h to remove any residual molecules that might have been trapped in the pores before analysis. In order to obtain pore volume, surface properties, and pore structure for both MOFs, nitrogen adsorption-desorption isotherms were recorded at 77 K. The adsorption isotherm of MIL-53(Fe) is of type IV with an H3-type hysteresis loop according to Fig. 4d indicating a microporosity. The surface area and the total pore volume obtained from BET studies of the sorbent were 13.614 and 0.103 cm^3/g, respectively. In addition, the average pore size was calculated to be 30.263 nm. This suggests a moderate amount of mesoporosity in the synthesized MIL-53(Fe) [47]. On the contrary, the thio-rich double-linker MIL-53(Fe) exhibited considerably superior textural characteristics. The double-linker MIL-53(Fe) N_2 adsorption–desorption isotherm, as shown in Fig. 4d, suggests capillary condensation in mesopores due to the sharp increase at elevated relative pressures. BET studies indicated that the total surface area is 18.37 m^2/g and the total pore volume is 0.134 cm^3/g. The mean pore size was also calculated to be 29.168 nm. Vast BET quantitative findings with a fine detail were shown in Table S1. Very importantly, increased total surface area along with increased total pore volume in the thio-rich double- linkers MIL-53 (Fe), since these factors provide space for the adsorption of not just diffusion but also heavy metal cations, and thus develops a greater pool of possibilities among interaction with the functional groups of the thio-rich linker-bonded MIL-53(Fe). The features of their structure greatly enhance the capacity of the adsorbent toward metals such as Pb (II) and Cd (II) from water samples.

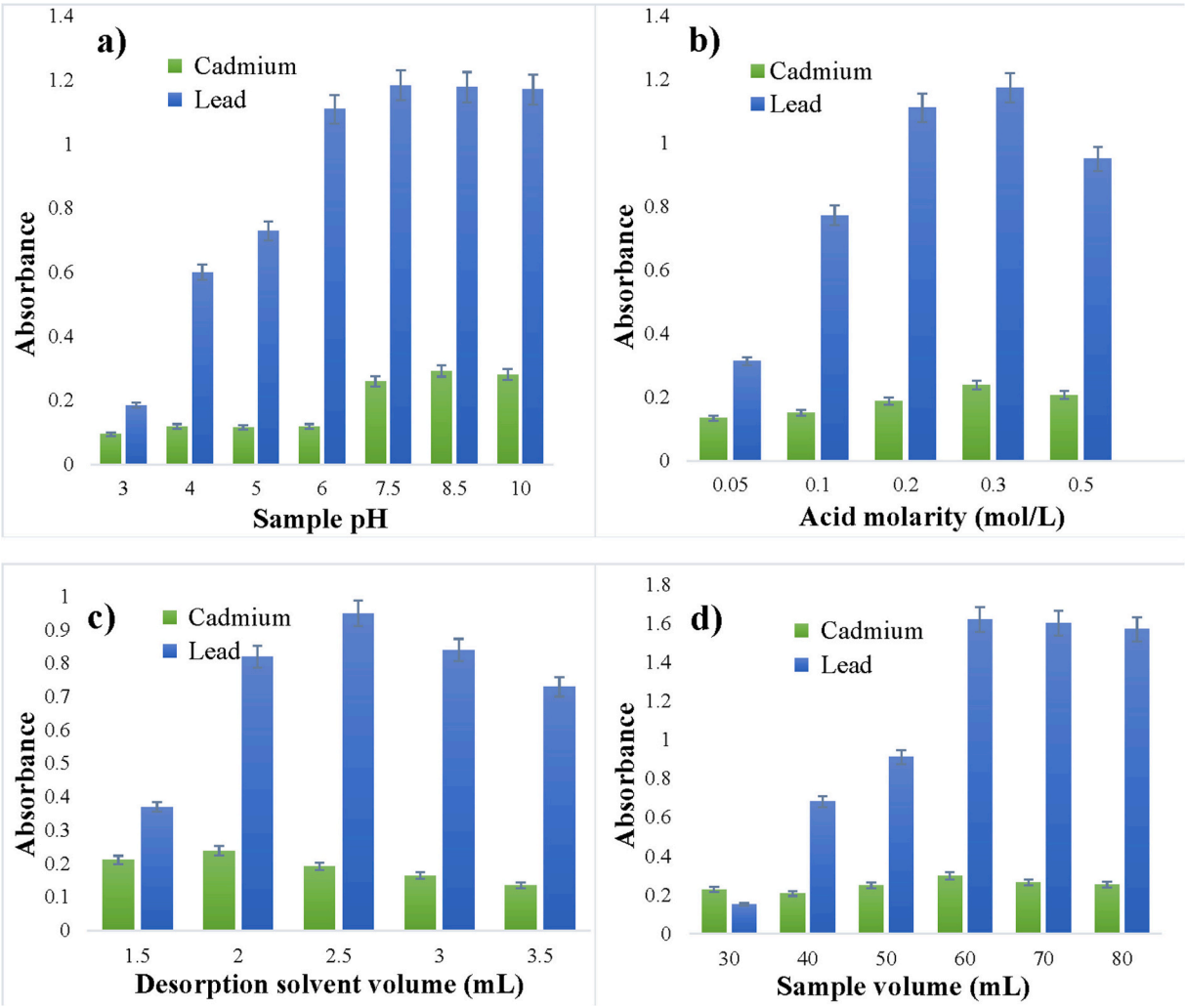

Fig. 5. Optimization of four key parameters affecting the extraction procedure. (a) pH, (b) acid concentration of desorption solution, (c) desorption solvent volume, (d) sample volume.

3.2. Optimization of the extraction method

3.2.1. Sample pH

The adsorptions of metal ions are highly pH-dependent; thus it is one of the most important factors controlling the adsorption reactions. Actually, pH changes can alter the structural composition and surface charge of the sorbent and, consequently, affect the chemical property and speciation of the adsorbate [48]. The effect of pH on the adsorption capacity of thio-rich double-linker MIL-53(Fe) sorbent has been studied in a pH range of 3.0–10.0 in an attempt to find an optimum pH for extracting Cd (II) and Pb (II) from natural water. As shown in Fig. 5a, the adsorption efficiency of Pb (II) increases exponentially from pH 3.0 to pH 7.5, after which it flattens out and reaches a plateau in the pH range of 7.5–10.0. The thio-rich double-linkers MIL-53 (Fe) surfaces exist as more preferable for Pb (II) coordination under nearly neutral to mildly alkaline conditions beyond possibly improved metal-ligands contacts and deprotonation of their functional groups. However, cadmium continues to be preferentially taken up to a steadily increasing maximum, as set at pH 8.5. At low pH, the binding of metals is suppressed by competing against the H^+ ions at the interface, while at higher pH levels, selective interaction with the MOF limits possibilities for precipitation of metal hydroxides. On the basis of these observations, a pH range of 7.5 and 8.5 was used for monitoring extraction of Pb (II) and Cd (II) from different environmental water samples.

3.2.2. Acid concentration of desorption solution

A variety of concentrations of nitric acid, from 0.05 to 0.5 mol L^{-1}, were assessed in order to study the effect of acid concentration as desorption solvent for the heavy metals under investigation. With increasing acid concentration in the case of the thio-rich double-linker MIL-53(Fe), improved metal adsorption was observed as illustrated in Fig. 5b. Increasing the acid concentration from 0.05 to 0.3 mol L^{-1} increased the desorption efficiency for Pb (II) and Cd (II), which constitutes the optimal desorption conditions. Extraction of metals at 0.5 mol L^{-1} was decreased due to interference of excess acid, which would likely affect adsorption. It can be concluded that the optimal dilution for desorbing Cd (II) and Pb (II) remains nitric acid at 0.3 mol L^{-1}. Higher acid concentration may influence surface properties of the adsorbent and reduce adsorption efficiency and stability [49].

3.2.3. Desorption solvent Volume

In desorption with thio-rich double-linker MIL-53 (Fe) as sorbent in PT-μSPE method, volume of desorption solvent played a major role in signal intensity and determining recovery efficiency of Pb (II) and Cd (II). Different volumes (from 1.5 to 3.5 mL) of 0.3 mol L^{-1} nitric acid were tried to study the influence. In Fig. 5c, it is noted that as the volume of desorption solvent was raised from 1.5 to 2.5 mL, there was an increase in the Pb (II) signal; however, with regard to Cd, desorption improved at around 2.0 mL. After 3.0 mL, however, both metals have very slight declines in signal intensity. The optimum desorption volume for Pb (II) is thus concluded to be 2.5 mL, while only 2.0 mL is found sufficient for Cd (II). The lack of use of chelating agents or any other reagents for metal extraction and desorption in this study, where only aqueous nitric acid solution is used for desorption, is in accordance with the principles of green chemistry.

3.2.4. Sample volume

A major parameter affecting the preconcentration factor in an extraction technique is sample volume [50]. To determine the optimal volume for adsorption of Pb(II) and Cd(II) using novel thio-rich double linkage MIL-53(Fe) as a sorbent in PT-μSPE, different sample volumes were tested as shown in Fig. 5d. Results showed an increase in sample volume from 30.0 to 80.0 mL greatly enhanced metal adsorption indicating improved extraction efficiency. Above 60.0 mL, adsorption plateaued suggesting that equilibrium had been reached, hence a further increase in sample volume did not enhance the adsorption signal. Thus, the sample volume of 60.0 mL was deduced to be the optimal volume for high extraction efficiency, minimum reagent consumption, and short time for analysis. Compared to conventional extraction techniques, this one offers a more favorable large sample volume in much less time, thereby increasing overall sensitivity.

3.2.5. Point of zero charge pH (pH_{pzc})

The pH value at which the total concentration of anions equals that of cations in a particular material is called the point of zero charge (pHpzc) [51]. The pHpzc of synthesized material is approximately calculated to be 5.5 as indicated in Fig. 6a. Above this pHpzc, the thio-rich double-linker MIL-53(Fe) surface becomes negatively charged, which could lead to the electrostatic attraction of the cationic species like Pb (II) and Cd (II) [52]. At pH values below 5.5, the surface will possess a positive charge, thereby favoring the electrostatic repulsion of the Pb (II) and Cd (II). The incorporation of thiol groups (–SH) into the (MOF) framework plays a significant role in increasing the selectivity of the sorbent for soft acid metal ions such as Pb (II) and Cd (II) via specific chemical interactions. The current study has involved calculating pHpzc of the synthesized thio-rich double-linker MIL-53(Fe) by using the immersion technique, meanwhile altering the pH for each of seven 0.1 mol L^{-1} sodium nitrate solutions. The alterations in pH were (3.0, 4.0, 5.0, 6.0, 7.5, 8.5, and 10.0) for every solution taken in 7.0 mL volumes. Each came with a total of 30.0 mg of this new double-liganded MIL-53(Fe) and the resulting suspension was shaken for a day. After equilibration, every final pH was registered, and differences between initial and final pH were determined. The pHpzc of the thio-rich double-linker MIL-53 (Fe) was determined using the point of intersection along the horizontal axis from the plotted data. It was taken to be the pH extraction optimized for the sorbent under study ranging between 6 and 10.

3.2.6. Comparison of MIL-53(Fe) and thio-rich double-linker MIL-53(Fe)

To examine the influence of the thio-functionality and the double-linker strategy on extraction efficiency of MIL-53(Fe) for target heavy metals of concern, two sorbents, i.e. pure MIL-53(Fe) and thio-rich double-linker MIL-53(Fe), were prepared and packed into the pipette tip and used for extraction of Pb (II) and Cd (II) from the water sample under identical conditions. The thio-rich double-linker MIL-53(Fe) showed dramatically enhanced extraction efficiency for both Cd (II) and Pb (II) compared to pristine MIL-53(Fe), as shown in Fig. 6b. This improvement is assumed to be due to the presence of functional groups containing donor atoms of sulfur and nitrogen capable of strongly coordinating heavy metal ions like Pb (II) and Cd (II). Besides, the existence of a second linker will change the pore environment and increase the surface reactivity, which will enhance adsorption performance even more. Therefore, thio-rich double-linker MIL-53(Fe) was found to be more efficient in extraction and provided lower detection limits as compared to the traditional single-linker MIL-53(Fe).

3.2.7. Adsorption isotherms

Figs. 7a and b indicate the adsorption isotherms of lead and cadmium onto the thio-rich double-linker MIL-53(Fe) and the initial MIL-53(Fe) for target metals concentrations varying from 0.1 to 50 mg L^{-1} for 2 h. The adsorption isotherms of both thio-rich double-linker MIL-53(Fe) and MIL-53(Fe) agree with each other regarding the trend. The adsorption capacity of Pb (II) and Cd (II) increased up to the equilibrium concentrations of Pb (II) and Cd (II) and, thereafter, decreased with an increase in equilibrium concentrations of Pb (II) and Cd (II). Higher adsorption capacity of Pb (II) and Cd (II) was, however, recorded for thio-rich double-linker MIL-53(Fe) compared to MIL-53(Fe), which truly highlights the significant role of the bonded sulfur groups in the adsorption of Pb (II) and Cd (II). The adsorption isotherm data were analyzed using the Langmuir model [37].

$$\frac{C_e}{Q_e} = \frac{1}{Q_m K_L} + \frac{C_e}{Q_m}$$

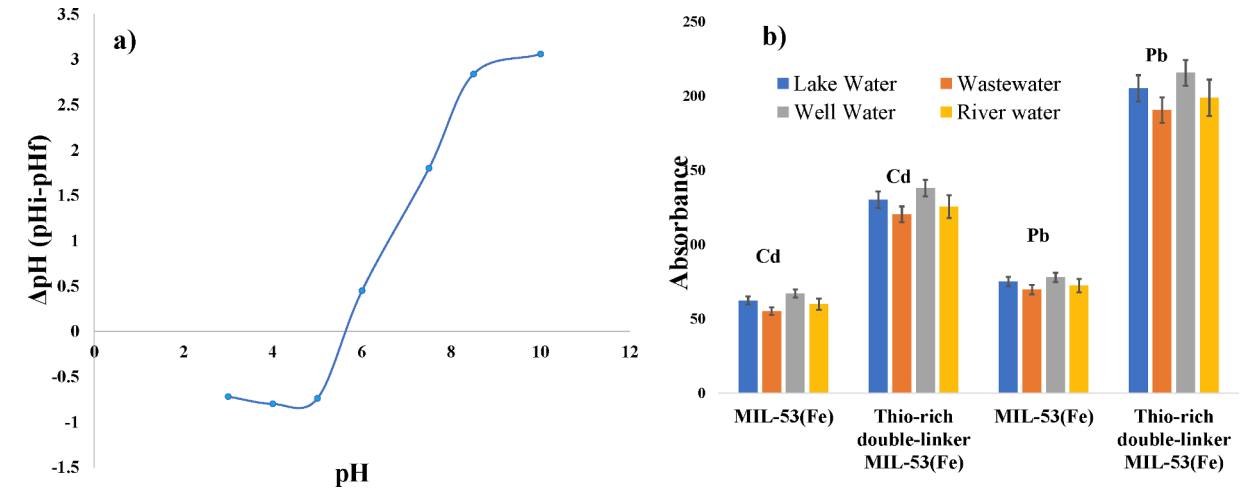

Fig. 6. (a) Point of zero charge for thio-rich double-linker MIL-53 (Fe). (b) Comparison between pure MIL-53(Fe) and thio-rich double-linker MIL-53(Fe) as sorbents in PT-μSPE.

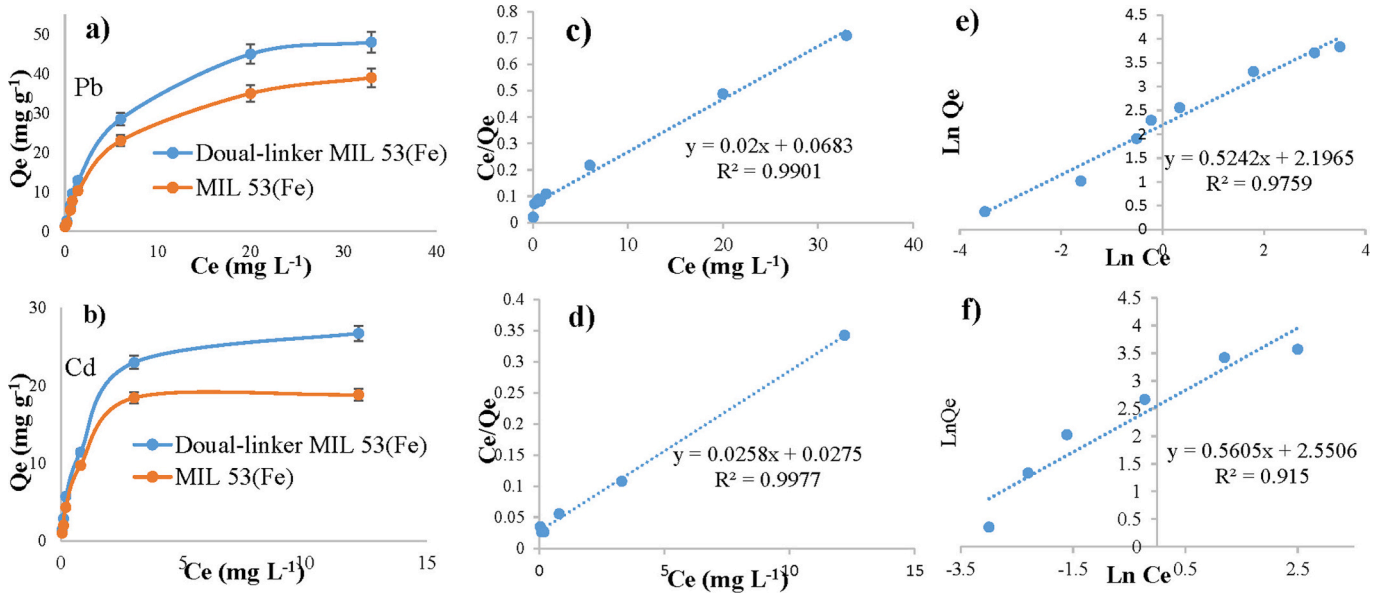

Fig. 7. Isothermal adsorption curves of thio-rich double-linker MIL-53 (Fe) for Pb(II) (a) and for Cd(II) (b), Langmuir isotherms adsorption model curves for Pb(II) (c) and for Cd(II) (d), and Freundlich isotherms adsorption model curves for Pb(II) (e) and for Cd(II) (f).

Ce (mg L^{-1}) being the equilibrium concentration of metals, Qe (mg g^{-1}) being the amount of metals adsorbed during the equilibrium, Qm (mg g^{-1}) being the maximum sorption of Pb (II) and Cd (II), and K_L (Lmg^{-1}) being the Langmuir constant. The linear plot of (Ce/Qe) versus Ce are given in Fig. 7c and d. The slope and x-intercept can be used to calculate the values of Qm and K_L (Table 2). The data fits well with Langmuir isotherm due to the R2 ≥ 0.99, while the Freundlich isotherm fits poorly (Fig. 7a and f) [53], which supports the conclusion that the adsorption of Pb (II) and Cd (II) onto the thio-rich double-linker MIL-53 (Fe) is essentially a monolayer adsorption (Table 2). Maximum adsorption capacities calculated for thio-rich double-linker MIL-53(Fe) are 50 mg g^{-1} for Pb (II) and 38.8 mg g^{-1} for Cd (II), which are greater than those of MIL-53(Fe), suggesting that the sulfur groups of thio-rich double-linker MIL-53(Fe) enhance the adsorption capacity for Pb (II) and Cd (II). The capacity of coordination differs with the thio-rich double-linker MIL-53(Fe) adsorption sites for M (II), which can again be explained by soft acid-base theory and hard acid-base theory. The concept of hard and soft acids and bases holds that a soft acid forms a stable complex with a soft base. While Pb (II) is defined as a borderline acid, Cd (II) is classed under soft acids. Similarly, -SH is categorized under soft bases while -COOH and -NH are considered hard bases. Therefore, Cd (II) tends to adsorb at the active -SH sites, whereas Pb (II) is more likely to adsorb at the -NH and -COOH sites [25]. This trend, whereby the adsorption capacity of thio-rich double-linker MIL-53(Fe) for Cd (II) is greater than for Pb (II), is partly due to the presence of thiol and -NH groups in addition to -COOH in thio-rich double-linker MIL-53(Fe). On the contrary, MIL-53(Fe) contains only -COOH (Fig. 7a

Table 2
. Langmuir and Freundlich adsorption isotherms fitting parameters of Pb (II) and Cd(II) on thio-rich double-linker MIL-53 (Fe).

Analytes	Langmuir			Freundlich		
	Q_m (mg g^{-1})	K_L (L mg^{-1})	R^2	K_F (mg g^{-1})	1/n	R^2
Pb	50	0.292	0.9901	8.93	0.5242	0.9759
Cd	38.8	0.938	0.9977	12.8	0.5605	0.9150

and b).

3.2.8. Figures of merit

The analytical performance of μ-SPE method was validated to determine Pb (II) and Cd (II) content in water samples using thio-rich double-linker MIL-53(Fe) as the sorbent. Summary of significant analytical figures of merit under ideal conditions, as presented in Table 3. Under the concentration ranges of 0.2–55.0 μg L^{-1} for Pb (II) and 0.04–20.0 μg L^{-1} for Cd (II), good linearities were exhibited by the method. Based on the 3S/N (signal/noise) the limits of detection (LOD) were found to be 0.01 μg L^{-1} for Cd (II) and 0.05 μg L^{-1} for Pb (II). Limitations of quantifications (LOQ) were calculated to be 0.04 μg L^{-1} for Cd (II) and 0.2 μgL^{-1} for Pb (II) based on 10 S/N standard. Good precision was obtained with intra-day relative standard deviations (RSD %, $n = 5$) in the concentration ranges of 5.0–5.9 % for Pb (II) and 3.7–4.0 % for Cd (II) and inter-day ($n = 3$) was 4.8–6.3 %. Within the examined ranges, the linearity of the method is confirmed by correlation coefficients (r^2) of 0.993 for Cd (II) and 0.992 for Pb (II) which affirms its reliability. Good enrichment factor (EF) in the range 20–26 was achieved.

3.2.9. Analysis of real sample

The performance evaluation of the newly synthesized thio-rich double-linker MIL-53(Fe)-based PT-μSPE method was done through analyzing the concentrations of Pb (II) and Cd (II) from various real environmental water sources collected from lakes, rivers, underground, and wastewaters in Duhok city. GFAAS was used to measure the levels of these metals in the samples collected, and the results are given in Table 4. Both metals were recorded at detectable levels in unspiked samples, ranging from 4.5 to 13.1 μg L^{-1} Pb (II) and 0.9 to 4.6 μg L^{-1} Cd (II), confirming the contamination of these metals in the local aqueous environment. To investigate the recoveries and validity of this method, the following spiking concentrations of Pb (II) (5.0 and 20.0 μg L^{-1}) and Cd (II) (1.0 and 5.0 μg L^{-1}), respectively, were carried out. The above method was also applied for the determination of Cd (II) and Pb (II) in Standard Reference Material for natural water (SRM 1640a, National Institute of Standards and Technology; USA). The relative recovery of spiked samples ranged from 90.0 % to 112.0 % for cadmium and from 88.0 % to 110.0 % for lead. Recovery for the validated reference material was 105 % for cadmium and 95 % for lead. This is justifiable under the following definition of acceptability: the relative recovery rate of spiked samples lies between 80.0 % and 120.0 % [54,55]. Indeed, all recoveries were within the allowable limit for trace-level analysis, confirming the applicability of the method to complex environmental matrices. The Pb (II) and Cd (II) concentrations in effluents from an unspiked water sample and in standard reference material (SRM 1640a) were determined using ICP-MS and the proposed method, respectively, as shown in Table 4. The results were statistically analyzed using the paired student *t*-tests, and none of the differences were statistically significant ($P > 0.05$). This means that there was an acceptance or concurrence among the two methods' results, which attests to the accuracy and reliability of the results obtained by this method in the present study. In addition, the relative percentage errors calculated were from 3.4 to 7.1 %, values that are acceptable for method validation [56,57].

3.2.10. Interferents

The water environments contain a plethora of mineral ions, which may adsorb onto the sulfur present in the MOF structure and, hence, be extracted simultaneously along with the targeted ions within the desired pH range [58] The effect of common, coexisting ions on the recovery of Cd (II) and Pb (II) from real water samples was investigated. For this purpose, 60 mL each of Cd (II) and Pb (II) standard solutions (1.0 and 5.0 μg L^{-1}) were spiked with different quantities of interfering ions, which were studied individually for each ion according to the recommended methods. A change in recovery of more than ±5 % was set as the interference criterion for that specific ion. Results are summarized in Table S2.

3.2.11. Reusability

The stability of the synthesized MOF was tested for 100 cycles of extraction under optimized conditions. PT - μSPE applied with cadmium and lead concentrations of 25.0 μgL^{-1} was used to evaluate the extraction performance of the reused sorbent after these cycles. As seen in Fig. S1, there was no significant change in extractability for cadmium and lead using the thio-rich, double linker MIL-53(Fe) up to 60 cycles, with a decreasing trend thereafter (i.e., based on GF-AAS adsorption of cadmium and lead). Thus, this confirms that the synthesized adsorbent has good stability under the optimized experimental conditions.

3.2.12. Comparison of thio-rich MOF-PT-μSPE and other related methods

The effectiveness of PT-μSPE method for determination of Pb (II) and Cd (II) levels in environmental water samples was assessed using a newly synthesized thio-rich double linker MIL-53(Fe) as the sorbent. As can be seen in Table S3, this method's analytical performance, including LOD, LOQ, linear range, r^2, and RSD%, is as good as or even better than that of many previously reported extraction procedures. The method has good reproducibility with RSDs of 5.9 % for lead and 4.0 % for cadmium. The double-linker MIL-53(Fe) MOF used for such purpose shows high capability for the pre-concentration of Pb (II) and Cd (II) ions in environmental water matrices using it as a sorbent. This sorbent has major advantages compared to conventional ones because of functionalization with terephthalic acid and 2-mercapto-2-thiazoline further gives nitrogen and sulfur donor atoms that tightly bind heavy metal ions. In addition, thiol groups increase selectivity and binding capacity; their porous structure and high surface area allow mass transfer and adsorption efficiency. While such substitutes are contributing to sensitive detection, thio-rich double linker MIL-53(Fe) showed better performance than MIL-53(Fe) sorbents under sensitivity and even low detection limits comparable to those above many reported methods.

4. Conclusion

Before real samples can be analyzed for heavy metals at trace concentrations, extraction and preconcentration must be performed efficiently; in the μSPE method, this lies in the hands of chemical properties and adsorption capacity of the adsorbent. Among new adsorbents, it is stipulated that MOF could be effective by changing functional groups and structure. In this study, for the first time, 2-mercapto-2-thiazoline was introduced as the second linker into the MIL-53(Fe) structure, increasing adsorption capacity for Pb (II) and Cd (II) because of the presence of two sulfurs and one -NH. This also enhanced extraction

Table 3
Analytical figure of merit of PT- μSPE method for determination of Pb (II) and Cd (II) in water samples.

Sample	Metals	LOD (μg L^{-1})	LOQ (μg L^{-1})	L.R (μg L^{-1})	r^2	Intra-day RSD% (n = 5)		Inter-day RSD%(n = 3)	EF
Tap water	Pb	0.05	0.2	0.2–55	0.992	5.0 μg L^{-1}	20.0 μg L^{-1}	20.0 μg L^{-1}	
						5.9	5.0	6.3	26
	Cd	0.01	0.04	0.04–20	0.993	1.0 μg L^{-1}	5.0 μg L^{-1}	5.0 μg L^{-1}	
						4.0	3.7	4.8	20

Table 4
Determination of Pb (II) and Cd (II) in real samples and relative recoveries of spiked samples.

Samples	Pb						Cd					
	Added (μg L^{-1})	Found (μg L^{-1}) (mean ± SD, n = 3)[a]	t-test[b]	RR%	ICP-MS Validation	Relative Error%	Added (μg L^{-1})	Found (μg L^{-1}) (mean ± SD, n = 3)[a]	t-test[b]	RR%	ICP-MS Validation	Relative Error%
Lake water	0	5.6 ± 0.1	–	–	5.3	5.7	0	1.1 ± 0.04	–	–	1.04	6.0
	5.0	11.1 ± 0.5	1.7	110.0	–	–	1.0	2.2 ± 0.07	2.5	110.0	–	–
	20.0	23.2 ± 1.4	2.9	88.0	–	–	5.0	6.0 ± 0.18	0.9	98.0	–	–
River water	0	9.5 ± 0.4	–	–	9.0	5.5	0	0.9 ± 0.03	–	–	0.85	5.8
	5.0	14.5 ± 0.7	0	100.0	–	–	1.0	1.9 ± 0.07	0	100.0	–	–
	20.0	27.8 ± 1.2	2.4	91.5	–	–	5.0	5.9 ± 0.19	0	100.0	–	–
Waste water	0	4.5 ± 0.2	–	–	4.2	7.1	0	4.6 ± 0.18	–	–	4.2	4.7
	5.0	9.3 ± 0.4	0.9	96.0	–	–	1.0	5.5 ± 0.19	0.9	90.0	–	–
	20.0	25.6 ± 1.4	1.3	105.5	–	–	5.0	10.0 ± 0.33	2.1	108.0	–	–
Well water	0	13.1 ± 0.7	–	–	12.6	3.9	0	3.0 ± 0.12	–	–	2.9	3.4
	5.0	18.2 ± 1	0.2	102.0	–	–	1.0	4.1 ± 0.14	1.2	110.0	–	–
	20.0	32.2 ± 1.7	0.9	95.5	–	–	5.0	8.6 ± 0.35	2.9	112.0	–	–
SRM 1640a	Certificate value 12.1	11.5 ± 0.6	1.7	95.0	-	4.9	Certificate value 3.99	4.2 ± 0.15	2.4	105.0	-	5.2

%RE (Percent relative error) = 100 × (|measured value − actual value|)/ actual value. Measured value: Cd (II) concentration obtained by applying the developed methodology. Actual value: Cd (II) and Pb (II) concentration found by ICP-MS.
[a] mean ± standard deviation based on three replicates.
[b] Tabulated t-value for 2 degrees of freedom at 95 % confidence level is 2.9.

efficiencies for Pb (II) and Cd (II), by solvent desorption, due to the change in the structure and increase in pore volume of the thio-rich double-linker MIL-53(Fe) adsorbent. The thio-rich dual-linker MIL-53 (Fe) was packed inside the pipette tip as adsorbent material for extraction and determination of Pb and Cd. The reusability of thio-rich dual-linker MIL-53(Fe) allows it to be used more than 60 cycles for the PT-μSPE technique because of its better chemical stability and easier desorption of target metals. Because only acid aqueous solution was used for adsorption and desorption, it fulfills the green chemistry targets. Such encouraging results point toward the possibility of the use of this ligand in future research in other MOFs for the subsequent adsorption and desorption of metals and other pollutants.

CRediT authorship contribution statement

Qaissar Guti Omo: Writing – original draft, Validation, Project administration, Methodology, Formal analysis. **Soleyman Moinfar:** Writing – review & editing, Validation, Supervision, Project administration, Data curation, Conceptualization.

Declaration of competing interest

The authors declare that they have no known competing financial interests or personal relationships that could have appeared to influence the work reported in this paper.

Acknowledgments

The authors gratefully acknowledge the financial support of the University of Zakho, Iraq.

Appendix A. Supplementary data

Supplementary data to this article can be found online at https://doi.org/10.1016/j.microc.2025.116339.

Data availability

No data was used for the research described in the article.

References

[1] S.S. Sonone, S. Jadhav, M.S. Sankhla, R. Kumar, Water contamination by heavy metals and their toxic effect on aquaculture and human health through food chain, Lett Appl NanoBioScience 10 (2020) 2148–2166, https://doi.org/10.33263/LIANBS102.21482166.
[2] Z. Zuo, H. Zhang, S. Gao, C. Wang, W.-T. Chen, G. Hu, Recent progress in porous organic frameworks for electrochemical sensing of environmental pollutants, J. Environ. Chem. Eng. 12 (2024) 113263, https://doi.org/10.1016/j.jece.2024.113263.
[3] M. Adnan, B. Xiao, P. Xiao, P. Zhao, S. Bibi, Heavy metal, waste, COVID-19, and rapid industrialization in this modern era—fit for sustainable future, Sustainability 14 (2022) 4746, https://doi.org/10.3390/su14084746.
[4] X. Zhang, L. Yan, J. Li, H. Yu, Adsorption of heavy metals by l-cysteine intercalated layered double hydroxide: kinetic, isothermal and mechanistic studies, J. Colloid Interface Sci. 562 (2020) 149–158, https://doi.org/10.1016/j.jcis.2019.12.028.
[5] B. Tripathy, A. Dash, A.P. Das, Detection of environmental microfiber pollutants through vibrational spectroscopic techniques: recent advances of environmental monitoring and future prospects, Crit. Rev. Anal. Chem. 54 (2024) 1925–1935, https://doi.org/10.1080/10408347.2022.2144994.
[6] Organization WH, Guidelines for Drinking-Water Quality: Incorporating the First and Second Addenda, World Health Organization, 2022.
[7] J. Zhang, X. Li, L. Guo, Z. Deng, D. Wang, L. Liu, Assessment of heavy metal pollution and water quality characteristics of the reservoir control reaches in the middle Han River, China. Sci Total Environ 799 (2021) 149472, https://doi.org/10.1016/j.scitotenv.2021.149472.
[8] A. Demirak, M. Kocakaya, F. Keskin, Chemical fractions of toxic metals and assessment of risks on the environment and health in Mugla topsoils, Int. J. Environ. Sci. Technol. 19 (2022) 5631–5648, https://doi.org/10.1007/s13762-021-03547-0.
[9] X. Wang, Y. Xu, Y. Li, Y. Li, Z. Li, W. Zhang, et al., Rapid detection of cadmium ions in meat by a multi-walled carbon nanotubes enhanced metal-organic framework modified electrochemical sensor, Food Chem. 357 (2021) 129762, https://doi.org/10.1016/j.foodchem.2021.129762.
[10] A.C. Carneiro, J. Meneguin, P. dos Santos, M. Corazza, M.C. Prete, A.W. Rinaldi, et al., On-line Micro-packed column solid-phase extraction of cadmium using metal-organic framework (MOF) UiO-66 with posterior determination by TS-FF-AAS, J. Braz. Chem. Soc. 33 (2022) 958–968, https://doi.org/10.21577/0103-5053.20220049.
[11] S. Chen, J. Yan, J. Li, D. Lu, Dispersive micro-solid phase extraction using magnetic ZnFe2O4 nanotubes as adsorbent for preconcentration of co(II), Ni(II), Mn(II) and cd(II) followed by ICP-MS determination, Microchem. J. 147 (2019) 232–238, https://doi.org/10.1016/j.microc.2019.02.066.

[12] M. Soylak, T. Zorlu, F. Uzcan, Dispersive solid phase microextraction of cadmium at trace levels on Cu2O nanocubes from food and water samples prior to its FAAS detection, J. Food Compos. Anal. 143 (2025) 107545, https://doi.org/10.1016/j.jfca.2025.107545.
[13] H.R. Cadorim, M. Schneider, J. Hinz, F. Luvizon, A.N. Dias, E. Carasek, et al., Effective and high-throughput analytical methodology for the determination of Lead and cadmium in water samples by disposable pipette extraction coupled with high-resolution continuum source graphite furnace atomic absorption spectrometry (HR-CS GF AAS), Anal. Lett. 52 (2019) 2133–2149, https://doi.org/10.1080/00032719.2019.1596117.
[14] W.A. Khan, M.B. Arain, M. Soylak, Nanomaterials-based solid phase extraction and solid phase microextraction for heavy metals food toxicity, Food Chem. Toxicol. 145 (2020) 111704, https://doi.org/10.1016/j.fct.2020.111704.
[15] H.A.A. Almafrachi, N.E. Gümüş, Öcal İ. Çorak, Heavy metal bioaccumulation in fish: ımplications for human health risk assessment in ten commercial fish species from Konya, Türkiye. Int J Environ Sci Technol 22 (2025) 4065–4074, https://doi.org/10.1007/s13762-024-05875-3.
[16] M. Mohebbi, R. Heydari, M. Ramezani, Determination of Cu, Cd, Ni, Pb and Zn in Edible Oils Using Reversed-Phase Ultrasonic Assisted Liquid–Liquid Microextraction and Flame Atomic Absorption Spectrometry, J. Anal. Chem. 73 (2018) 30–35, https://doi.org/10.1134/S1061934818010069.
[17] H.U. Haq, A. Elik, G. Isci, M. Ekici, N. Gürsoy, G. Boczkaj, et al., Development of a vortex-assisted switchable-hydrophilicity solvent-based liquid phase microextraction for fast and reliable extraction of Zn (II), Fe (II), Pb (II), and cd (II) from various baby food products, Food Chem. 447 (2024) 139024.
[18] A. Bakhshi, S.M. Sorouraddin, M.R. Afshar Mogaddam, M.A. Farajzadeh, Continuous homogeneous liquid –liquid microextraction for the extraction of cd (II), cu(II), and Zn(II) ions from oil samples based on in-situ preparation of a deep eutectic solvent, J. Food Compos. Anal. 144 (2025) 107649, https://doi.org/10.1016/j.jfca.2025.107649.
[19] H.E.H. Ahmed, N. Güy, M. Soylak, Eco-friendly synthesis of CuO/g-C_3N_4/Fe_3O_4 nanocomposites for efficient magnetic micro-solid phase extraction (M-μ-SPE) of trace cadmium from food and water samples, Food Chem. 470 (2025) 142626, https://doi.org/10.1016/j.foodchem.2024.142626.
[20] M.E.I. Badawy, M.A.M. El-Nouby, P.K. Kimani, L.W. Lim, E.I. Rabea, A review of the modern principles and applications of solid-phase extraction techniques in chromatographic analysis, Anal. Sci. 38 (2022) 1457–1487, https://doi.org/10.1007/s44211-022-00190-8.
[21] J. Zolgharnein, F. Rajabalipour, Farahani S. Dermanaki, Indigo carmine dye adsorptive removal by polyethylene glycol-modified hydroxyapatite nanoparticles as an efficient adsorbent, Water Air Soil Pollut. 234 (2023) 210, https://doi.org/10.1007/s11270-023-06207-w.
[22] S.H. Hashemi, M. Kaykhaii, A. Jamali Keikha, E. Mirmoradzehi, Box-Behnken design optimization of pipette tip solid phase extraction for methyl orange and acid red determination by spectrophotometry in seawater samples using graphite based magnetic NiFe2O4 decorated exfoliated as sorbent, Spectrochim Acta Part A Mol Biomol Spectrosc 213 (2019) 218–227, https://doi.org/10.1016/j.saa.2019.01.049.
[23] P.V. Mane, R.M. Rego, P.L. Yap, D. Losic, M.D. Kurkuri, Unveiling cutting-edge advances in high surface area porous materials for the efficient removal of toxic metal ions from water, Prog. Mater. Sci. 146 (2024) 101314, https://doi.org/10.1016/j.pmatsci.2024.101314.
[24] F. Ayesh Alharthi, A.A. Abutaleb, M.M. Aljohani, M. Alshareef, Recent Progress in metal-organic frameworks (MOFs) for the detection and removal of heavy metal ions from water: a comprehensive review, Comments Inorg. Chem. 45 (2025) 245–282, https://doi.org/10.1080/02603594.2024.2360737.
[25] X. Zhang, Z. Zhai, X. Feng, H. Hou, Y. Zhang, Recent Advances of Metal–Organic Framework for Heavy Metal Ions Adsorption, Langmuir 40 (2024) 17868–17888, https://doi.org/10.1021/acs.langmuir.4c01757.
[26] Y. Zhou, J. Xiong, L. Wang, F. Li, H. Bai, S. Wang, et al., Multi-ligand strategy for enhanced removal of heavy metal ions by thiol-functionalized defective Zr-MOFs, J. Hazard. Mater. 479 (2024) 135723, https://doi.org/10.1016/j.jhazmat.2024.135723.
[27] D.-B. Zhou, Y.-B. Xiao, F. Han, Y.-N. Lv, L. Ding, W. Song, et al., Magnetic solid-phase extraction based on sulfur-functionalized magnetic metal-organic frameworks for the determination of methylmercury and inorganic mercury in water and fish samples, J. Chromatogr. A 1654 (2021) 462465, https://doi.org/10.1016/j.chroma.2021.462465.
[28] L. Fu, S. Wang, G. Lin, L. Zhang, Q. Liu, J. Fang, et al., Post-functionalization of UiO-66-NH2 by 2,5-Dimercapto-1,3,4-thiadiazole for the high efficient removal of hg(II) in water, J. Hazard. Mater. 368 (2019) 42–51, https://doi.org/10.1016/j.jhazmat.2019.01.025.
[29] X. Zhao, X. Gao, Y.-N. Zhang, M. Wang, X. Gao, B. Liu, Construction of dual sulfur sites in metal–organic framework for enhanced mercury(II) removal, J. Colloid Interface Sci. 631 (2023) 191–201, https://doi.org/10.1016/j.jcis.2022.10.153.
[30] C. Xu, M. He, B. Chen, B. Hu, Magnetic S-functionalized Nanoporous Zr-metal organic frameworks with defect-induced performance in hg(II) removal, ACS Appl. Nano Mater. 6 (2023) 17521–17530, https://doi.org/10.1021/acsanm.3c02692.
[31] D.R. Sáenz-García, A. Figuerola, G. Turnes Palomino, L.O. Leal, Cabello C. Palomino, Thiol-functionalized MIL-100(Fe)/device for the removal of heavy metals in water, Inorg. Chem. 62 (2023) 19404–19411, https://doi.org/10.1021/acs.inorgchem.3c01544.
[32] M. Kaykhaii, S.H. Hashemi, J. Gębicki, Applications of metal organic framework adsorbents for pipette-tip micro solid-phase extraction, TrAC Trends Anal. Chem. 1 (179) (2024) 117877, https://doi.org/10.1016/j.trac.2024.117877.
[33] M.R. Rezaei Kahkha, S. Daliran, A.R. Oveisi, M. Kaykhaii, Z. Sepehri, The mesoporous porphyrinic zirconium metal-organic framework for pipette-tip solid-phase extraction of mercury from fish samples followed by cold vapor atomic absorption spectrometric determination, Food Anal. Methods 10 (7) (2017) 2175–2184, https://doi.org/10.1007/s12161-016-0786-x.
[34] M. Abbaszadeh, A. Miri, M.R. Kahkha, Determination of cadmium in rice samples using amino-functionalized metal-organic framework by a pipette tip solid phase extraction, Analytical Methods in Environmental Chemistry Journal 5 (03) (2022) 70–79, https://doi.org/10.24200/amecj.v5.i03.208.
[35] F. Wu, D. Yuan, Q. Niu, D. Chen, X. Zhu, Metal-organic framework (MOF) materials and functionalization for targeted adsorption of pb and cd in wastewater: mechanisms, challenges, and future development prospects, Adv. Colloid Interf. Sci. 344 (2025) 103597, https://doi.org/10.1016/j.cis.2025.103597.
[36] C.M. Navarathna, N.B. Dewage, A.G. Karunanayake, E.L. Farmer, F. Perez, E. B. Hassan, et al., Rhodamine B adsorptive removal and photocatalytic degradation on MIL-53-Fe MOF/magnetic magnetite/biochar composites, J. Inorg. Organomet. Polym. Mater. 30 (2020) 214–229, https://doi.org/10.1007/s10904-019-01322-w.
[37] P. Han, Y. Xia, Thiol-functionalized metal-organic framework for highly efficient removal of bromate from water, J. Environ. Chem. Eng. 6 (2018) 3384–3391, https://doi.org/10.1016/j.jece.2018.03.045.
[38] T.T. Quang, N.X. Truong, T.H. Minh, N.N. Tue, G.T.P. Ly, Enhanced photocatalytic degradation of MB under visible light using the modified MIL-53(Fe), Top. Catal. 63 (2020) 1227–1239, https://doi.org/10.1007/s11244-020-01364-2.
[39] T. Li, X. Ba, X. Wang, Z. Wang, J. Yang, Y. Cui, et al., MIL-53(Fe)@γ-Al2O3 nanocomposites incorporated cellulose acetate for forward osmosis membranes of high desalination performance, Environ Eng Res 28 (2022), https://doi.org/10.4491/eer.2021.448, 210448–0.
[40] A.A. Ranchani, V. Parthasarathy, S. Mahalakshmi, R. Anbarasan, Facile synthesis of Fe nanospheres anchored aminoclay and its catalytic reduction of hazardous pollutants and oxidation activity, J. Dispers. Sci. Technol. 42 (11) (2021) 1640–1650, https://doi.org/10.1080/01932691.2020.1776129.
[41] M.A. Khabbaz, M.H. Entezari, Simple and versatile one-step synthesis of FeS2 nanoparticles by ultrasonic irradiation, J. Colloid Interface Sci. 15 (470) (2016) 204–210, https://doi.org/10.1016/j.jcis.2016.02.055.
[42] P.P. Singh, O.P. Agrawal, A.K. Gupta, Studies on 2-thiazolidinethione, 2, 4-thiazolidinedione and ethylene monothiocarbonate complexes of Sn (IV), Ti (IV) and Fe (II) halides, Inorg. Chim. Acta 1 (18) (1976) 19–23, https://doi.org/10.1016/S0020-1693(00)95579-8.
[43] M. Ghanbarian, S. Zeinali, A. Mostafavi, T. Shamspur, Facile synthesis of MIL-53 (Fe) by microwave irradiation and its application for robust removal of heavy metals from aqueous solution by experimental design approach: kinetic and equilibrium, Anal Bioanal Chem Res 7 (2020) 263–280, https://doi.org/10.22036/abcr.2019.172731.1319.
[44] B. Abdollahi, M. Zarei, D. Salari, Synthesis, characterization, and application of diethylenetriamine functionalized MIL-53(Fe) metal-organic framework for efficient as(V) removal from surface and groundwater, J. Solid State Chem. 311 (2022) 123132, https://doi.org/10.1016/j.jssc.2022.123132.
[45] A. Nikseresht, A. Daniyali, M. Ali-Mohammadi, A. Afzalinia, A. Mirzaie, Ultrasound-assisted biodiesel production by a novel composite of Fe(III)-based MOF and phosphotangestic acid as efficient and reusable catalyst, Ultrason. Sonochem. 37 (2017) 203–207, https://doi.org/10.1016/j.ultsonch.2017.01.011.
[46] P. Sinha, A. Datar, C. Jeong, X. Deng, Y.G. Chung, L.-C. Lin, Surface area determination of porous materials using the Brunauer–Emmett–teller (BET) method: limitations and improvements, J. Phys. Chem. C 123 (2019) 20195–20209, https://doi.org/10.1021/acs.jpcc.9b02116.
[47] M. Al Haydar, H. Abid, B. Sunderland, S. Wang, Metal organic frameworks as a drug delivery system for flurbiprofen, Drug Des. Devel. Ther. 11 (2017) 2685–2695, https://doi.org/10.2147/DDDT.S145716.
[48] S. Naeimi, H. Faghihian, Application of novel metal organic framework, MIL-53 (Fe) and its magnetic hybrid: for removal of pharmaceutical pollutant, doxycycline from aqueous solutions, Environ. Toxicol. Pharmacol. 53 (2017) 121–132, https://doi.org/10.1016/j.etap.2017.05.007.
[49] M.R. Abdi, N. Sarlak, Magnetic metal-organic frameworks for determination of heavy metals in different cosmetic products available in Iran market by flame atomic absorption spectroscopy, Anal Bioanal Chem Res 12 (2025) 11–25, https://doi.org/10.22036/abcr.2024.457668.2108.
[50] M.R. Sohrabi, Z. Matbouie, A.A. Asgharinezhad, A. Dehghani, Solid phase extraction of cd(II) and Pb(II) using a magnetic metal-organic framework, and their determination by FAAS, Microchim. Acta 180 (2013) 589–597, https://doi.org/10.1007/s00604-013-0952-4.
[51] S. Moinfar, G. Khayatian, L.A. Jamil, Semi-automated continuous sample drop flow microextraction with swift preconcentration and atomic absorption spectrometry determination of lead in water and apple leaves, J. Iran. Chem. Soc. 15 (2018) 2511–2518, https://doi.org/10.1007/s13738-018-1439-3.
[52] B.-L. Zhang, W. Qiu, P.-P. Wang, Y.-L. Liu, J. Zou, L. Wang, et al., Mechanism study about the adsorption of Pb(II) and cd(II) with iron-trimesic metal-organic frameworks, Chem. Eng. J. 385 (2020) 123507, https://doi.org/10.1016/j.cej.2019.123507.
[53] S. Fekri, Y. Mansoori, A. Khodayari, Nanocomposites of a new organosoluble polyetherimide and epoxide-functionalized magnetite for removal of co(II) ions: kinetic and thermodynamic investigations, Polym. Compos. 40 (2019) 3166–3181, https://doi.org/10.1002/pc.25165.
[54] https://www.aoac.org/aoac_prod_imis/AOAC_Docs/StandardsDevelopment/SLV_Guidelines_Dietary_Supplements.pdf.
[55] D. Romero-Estévez, G.S. Yánez-Jácome, K. Simbaña-Farinango, P.Y. Vélez-Terreros, H. Navarrete, Determination of cadmium and lead in tomato (Solanum

lycopersicum) and lettuce (Lactuca sativa) consumed in Quito, Ecuador. Toxicol Reports 7 (2020) 893–899, https://doi.org/10.1016/j.toxrep.2020.07.008.
[56] P.A. Avaca Gagliardi, L.P. Fernández, M.C. Talio, New analytical methodology for cadmium quantification by solid surface fluorescence in biological samples, Microchem. J. 219 (2025) 116070, https://doi.org/10.1016/j.microc.2025.116070.
[57] S. Hu, S. Zhang, J. Qin, K. Cai, C. Peng, L. Luo, et al., Simultaneous determination of lead and cadmium in water by metal oxide framework complex-modified glassy carbon electrodes, Microchem. J. 205 (2024) 111154, https://doi.org/10.1016/j.microc.2024.111154.
[58] S. Moinfar, G. Khayatian, Continuous sample drop flow-based microextraction combined with graphite furnace atomic absorption spectrometry for determination of cadmium, Microchem. J. 132 (2017) 293–298, https://doi.org/10.1016/j.microc.2017.01.031.